STOP 7

John Wakabayashi, 1329 Sheridan Lane, Hayward, CA 94544, wako@tdl.com,
http://www.tdl.com/~wako/

Soakies Grade Overlook Stop, Seneca Road, Lake Almanor Area

At this stop we can view features related to Quaternary volcanic history, stream incision, and faulting in this area. The Basalt of Rock Creek (~1 Ma) is exposed in the roadcut above where you will park along the Seneca road (a section of road known as Soakies Grade). The basal baked zone is easily seen in the roadcut. This steep baked zone overlies a thin zone of colluvium, that, in turn, overlies Paleozoic basement; this represents a buttress unconformity of the base of the flow against the old canyon wall. This is typical of the terrace-like remnants of basalt that occur in the North Fork Feather River canyon. More extensive remnants generally have a large wedge of colluvium on top of them and have stream gravels at their base. After looking at this basalt we can walk toward the northeast a bit along the road to get a view toward the Lake Almanor basin.

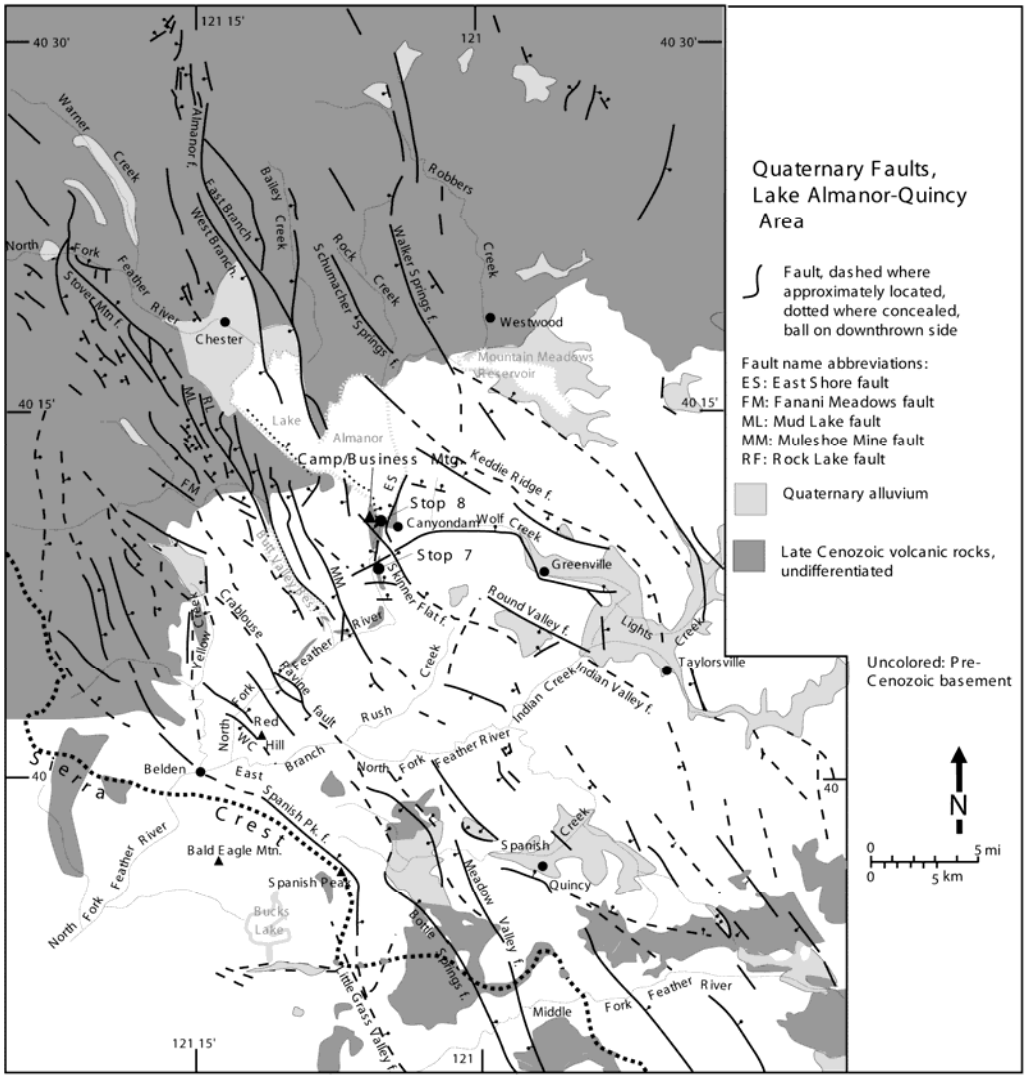

Figure 7-1: Quaternary faults of the Lake Almanor area. Adapted from Wakabayashi and Sawyer (2000).

Lake Almanor is a reservoir that floods a fault-bounded basin along some strands of the Mohawk Valley fault zone (Fig. 7-1). At this point we are at the northern limit of what is generally defined as the Sierra Nevada, as deposits of Plio-Pleistocene volcanic rocks cover essentially all older rocks to the north (the southern part of the Modoc plateau to the north and northeast or southern Cascades to the northwest).

In spite of the difference in rock types exposed at the surface, faulting along the Frontal fault system continues northward across the 'transition', part of a fault system that has been termed the Tahoe-Medicine Lake trough (Page et al., 1993). The Hat Creek fault, that forms the spectacular escarpment of the Hat Creek Rim north of this area, is part of the northern continuation of this fault system (e.g., Wills, 1990; Muffler et al., 1994). The Sierran-Modoc Plateau and Sierran-Cascades transitions are thus more a transition in rock types at the surface than a tectonic transition. Looking across the lake we observe a type of 'inverted topography' in which older volcanic rocks have been uplifted and younger volcanic rocks have flowed down channels cut into the older rocks. Across Lake Almanor, many of the highest areas are underlain by 2.2 Ma andesites. Younger basalt flows, the ~1 Ma Basalt of Rock Creek, ~0.6 Ma Basalt of Warner Valley, and ~0.4 Ma Basalt of Westwood, flowed down channels cut into older rocks (in the case of the 0.4 Ma basalts the rocks fill a channel cut into the 1 Ma rocks); these basalts flowed into the Almanor basin from the northwest, north, and northeast (Fig. 7-2). On the floor of the Almanor basin itself, beneath the lake and basin sediments, the volcanic flows likely overlie one another in stratigraphic sequence. Several of the basalts flowed through the Almanor basin and continued down the ancestral North Fork Feather River canyon, as will be discussed below.

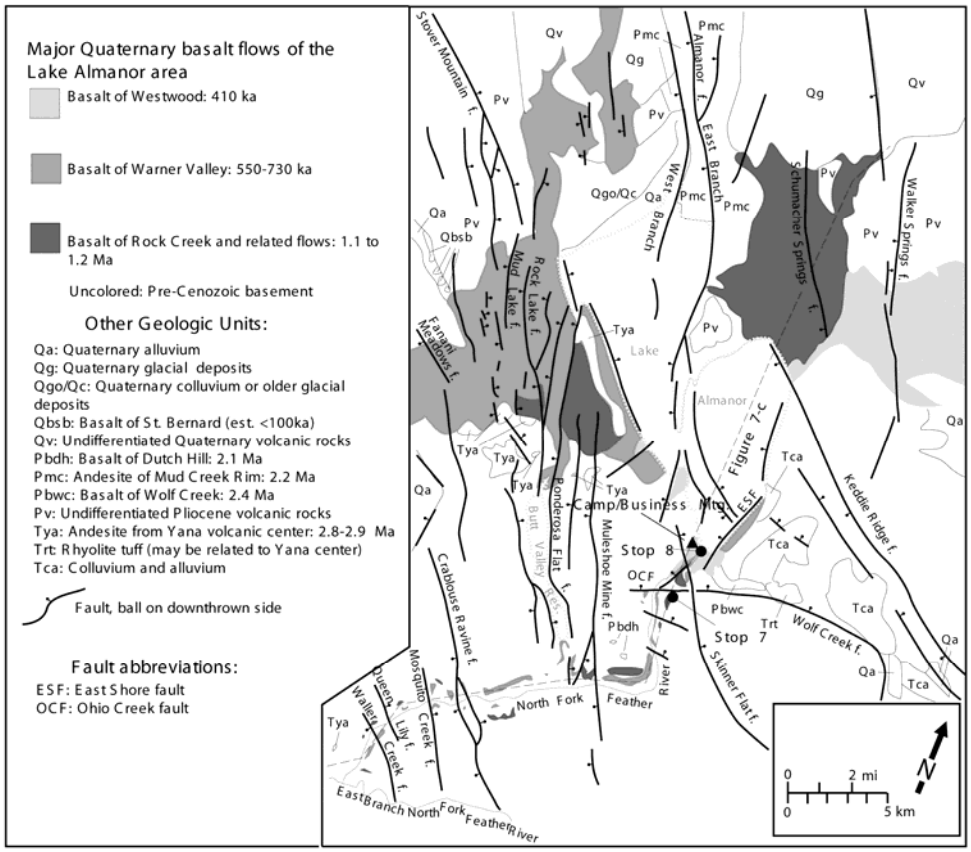

Figure 7-2: Plio-Pleistocene volcanic rocks, and Quaternary faults, Lake Almanor area. Adapted from Wakabayashi and Sawyer (2000).

At this viewpoint we are 'downstream' of the Almanor basin from the standpoint of the direction that the basaltic lavas flowed, yet we are significantly higher than the Almanor basin; because we are 'downstream' of the Almanor basin the elevation difference we see must be a consequence of faulting. The top of the basalt outcrop in the roadcut is 113 m higher than the high water level of Lake Almanor. The elevation difference between this remnant and the basin helps one visualize the vertical component of the faulting bounding this side of the Almanor basin (water depth is about 30 m). Note that the surface of this basalt in the Almanor basin is considerably lower than the bottom of the lake. In the basin, this basalt would be expected to be overlain successively by flows of the ~0.6 Ma Basalt of Warner Valley, the ~0.4 Ma Basalt of Westwood, and late Quaternary alluvial deposits that overlie these basalts in the basin.

Across the deep canyon of the North Fork Feather River to the north and northwest, we see a flat bench. The canyon walls reveal that the bench is underlain by Basalt of Westwood that overlies Basalt of Warner Valley; we will see this relationship at Stop 8. The Basalt of Westwood may not have made it much further downstream than the downstream limit of the bench, for it has not been found beyond that point. To the north of us, on our side (the east side) of the canyon, and partly blocking our view of the lake, is a wooded knob. This knob is capped with the Basalt of Warner Valley that overlies the Basalt of Rock Creek. The Skinner Flat fault, that passes northeast of this knob (backside of the knob relative to us), and a splay of the Ohio Creek fault, uplifts these exposures relative to Lake Almanor, and the bench on the west side of the river (Fig. 7-2). The relationships of the various basalts on each side of these faults suggest that the Skinner Flat fault may not have started significant movement until after the deposition of the Basalt of Westwood, whereas the main branch of the Ohio Creek fault may have moved after Basalt of Rock Creek time, but ceased movement before Basalt of Warner Valley time.

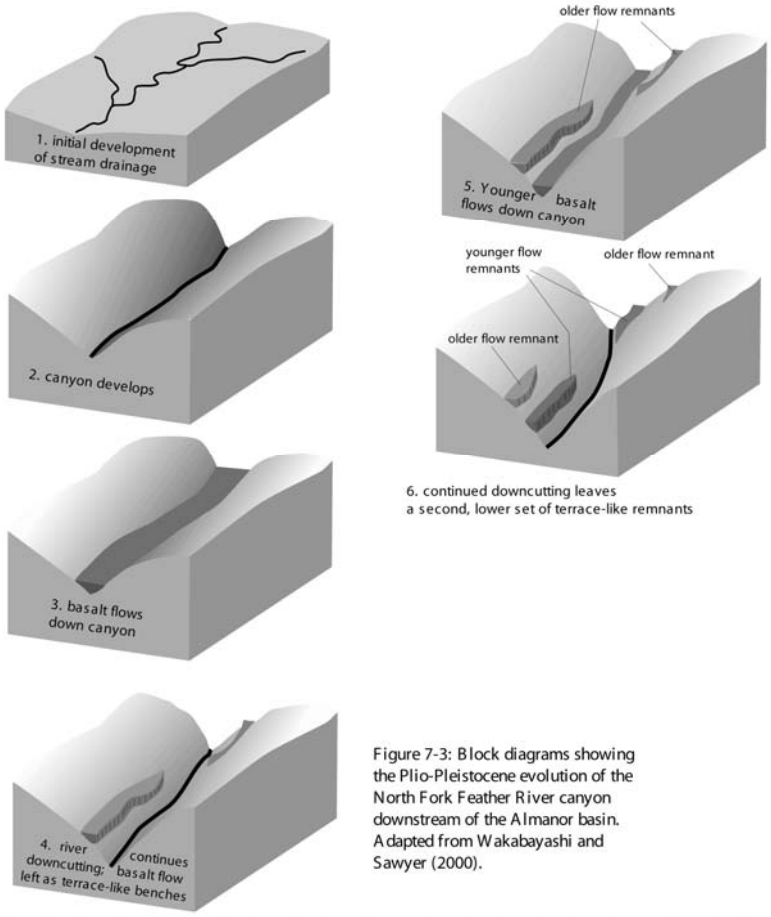

Figure 7-3: Block diagrams showing the Plio-Pleistocene evolution of the North Fork Feather River canyon downstream of the Almanor basin. Adapted from Wakabayashi and Sawyer (2000).

On the above-described wooded knob and the bench across the river basaltic units still overlie each other in normal stratigraphic fashion. Downstream of these outcrops, starting with the outcrops where we are stopped, an 'inverted' topographic series of basalt benches is seen, a consequence of successive river incision with periods of basalt flowing down the canyon (schematically shown in Fig. 7-3). The 'cross over' point is marked by the Ohio Creek fault that passes between the 'normal' stratigraphic sequences to our north and the outcrop that we are standing next to.

Now we will turn around and hike southeast up a dirt road onto the knoll on the east side of the main road, from which we can look downstream. From here we can see the river bend around a hill that has several prominent flat surfaces at different elevations. The lowest of the two flat surfaces are remnants of the 0.6 Ma Basalt of Warner Valley (lowest), and 1 Ma Basalt of Rock Creek (next bench up). Figure 7-4 was taken from a bit further down the canyon than our viewpoint, so that the lower bench

is more easily seen; it wraps around the bend in the canyon. Similar bench-like remnants exhibiting 'inverted' topographic relationships (oldest benches are highest) are present along the walls of the North Fork Feather River canyon as far downstream as the confluence of the North Fork with the East Branch North Fork. A canyon followed approximately the same course since at least 2.8 Ma, based on the oldest inset volcanic unit. The depth of the canyon at 2.8 Ma can be estimated by noting the position of the inset volcanic remnant of this age relative to erosion surfaces or basement topographic highs above it. The ages of the various terrace-like remnants of volcanic rocks in the North Fork Feather River canyon have been confirmed by Ar/Ar dating (Wakabayashi and Sawyer, 2000). Correlation of the terrace remnants in the canyon allow evaluation of vertical separation associated with faulting in the canyon (Fig. 7-5). Note that these are vertical separations on faults that appear to have a much larger strike-slip component (WLA, 1996). The Butt Valley fault zone, which has the largest vertical separation of any group of faults downstream of the Almanor dam area, appears to have the same separation of the Basalt of Warner Valley and the Basalt of Rock Creek, suggesting that faulting on these strands did not begin until after Basalt of Warner Valley deposition (~600 ka). Thus the two most significant fault zones in the North Fork Feather River canyon, the Skinner Flat fault and Butt Valley fault zones, both appear to have begun movement sometime after 600 ka. This start up of faulting may be a part of ongoing encroachment of the western margin of the Walker Lane or Frontal fault system into the Sierran block. Perhaps consistent with the immature state of the faults in this area is the fact that the Mohawk Valley fault zone/Frontal fault system in this area consists of many strands distributed over a zone 30 to 40 km wide. This zone is much narrower (about 10 km wide) south of Quincy.

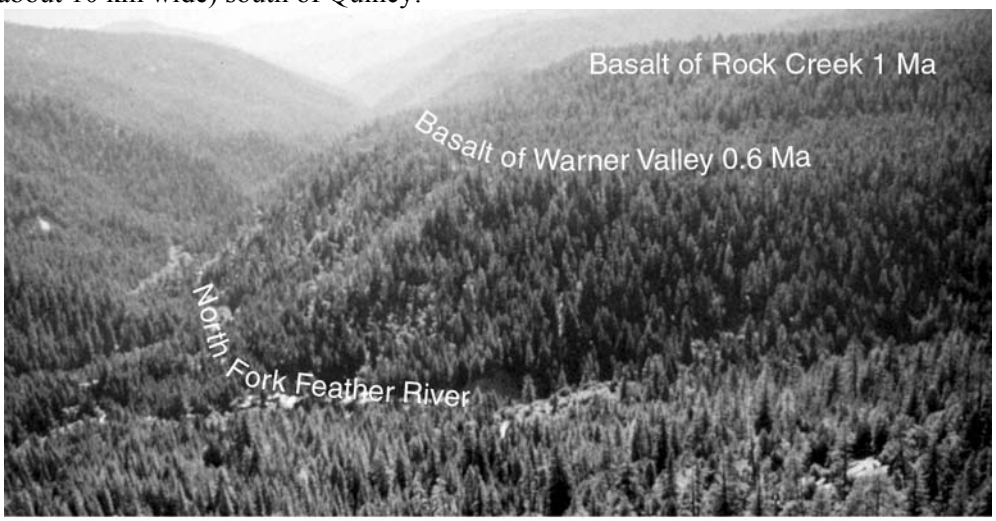

Figure 7-4. View down the North Fork Feather River Canyon from downstream of Stop 7, showing examples of terrace like remnants of Quaternary basalt flows in the canyon.

The terrace-like remnants of volcanic rocks in the North Fork Feather River canyon also allow estimation of incision rates. Incision relative to a volcanic unit can be measured in two ways: (1) from the top of the volcanic unit (includes the incision through the volcanic unit), referred to as 'total incision' (see also Fig. 10-1 for Stop 10), or (2) incision in rocks below the volcanic unit, referred to as 'basement incision' (Wakabayashi and Sawyer, 2001). For the various basalts in the North Fork Feather River canyon, incision can be measured between different times represented by the basalt flows. For example, basement incision between Basalt of Rock Creek and Basalt of Warner Valley time can be measured by the elevation difference between the base of a Basalt of Rock Creek flow remnant to the base of a Basalt of Warner Valley flow remnant along the same reach of the stream, whereas total incision between these two times can be measured by the elevation difference between the top of a Basalt of Rock Creek and the bottom of a Basalt of Warner Valley flow. The incision various between fault-bounded blocks is summarized in Table 7-1, and show diagramatically on Figure 7-5.

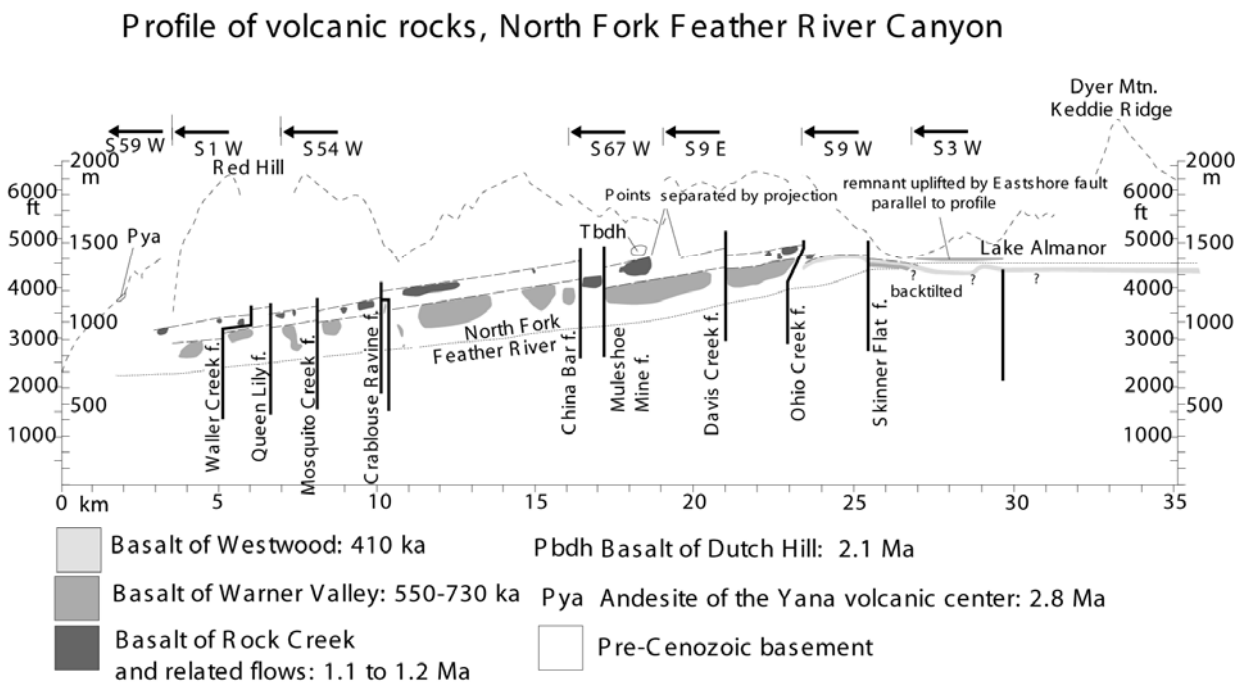

Figure 7-5: Profile of volcanic rocks, North Fork Feather River canyon projected to projection line shown in Fig. 7-2. Adapted from Wakabayashi and Sawyer (2000).

TABLE 7-1: INCISION RATE, NORTH FORK FEATHER RIVER, LAKE ALMANOR TO CONFLUENCE WITH EAST BRANCH NORTH FORK FEATHER RIVER

Fault Block or Reach of river	Total incision rate (mm/yr) with time interval; parentheses denote basement incision rate
Ohio Creek to Salmon Creek	0.57-0.73 Ma to present: 0.21-0.26 (0.096-0.12); 1.11-1.20 Ma to present: 0.22-0.24 (0.16-0.17); 1.11-1.20 Ma to 0.57-0.73 Ma: 0.31-0.52 (0.18-0.31)
Davis Creek to Meeker Bar	0.57-0.73 Ma to present: 0.30-0.38 (0.10-0.13); 1.11-1.20 Ma to present: 0.29-0.31 (0.24-0.25); 1.11-1.20 Ma to 0.57-0.73 Ma: 0.43-0.71 (0.33-0.54); 2.05 Ma to 1.11-1.20 Ma: 0.13-0.15 (0.052-0.058)
Butt Creek to Crablouse Ravine	0.57-0.73 Ma to present: 0.37-0.48 (0.15-0.19); 1.11-1.20 Ma to 0.57-0.73 Ma: 0.43-0.72 (0.31-0.51); 1.11-1.20 Ma to present: 0.32-0.34 (0.25-0.27)
Crablouse Ravine to Mosquito Creek	0.57-0.73 Ma to present: 0.28-0.36 (0.14-0.18); 1.11-1.20 Ma to 0.57-0.73 Ma: 0.32-0.54 (0.21-0.35)
Mosquito Creek to Queen Lily	0.57-0.73 Ma to present: 0.29-0.37 (0.067-0.086); 1.11-1.20 Ma to 0.57-0.73 Ma: 0.39-0.64 (0.31-0.51)
Waller Creek fault to East Branch confluence	0.57-0.73 Ma to present: 0.23-0.29 (0.12-0.15); 1.11-1.20 Ma to 0.57-0.73 Ma: 0.34-0.57 (0.24-0.40); 2.81 Ma to 1.11-1.20 Ma: 0.14 (0.082-0.086); 2.81 Ma to present: 0.17 (0.13)

STOP 8

John Wakabayashi, 1329 Sheridan Lane, Hayward, CA 94544, wako@tdl.com, http://www.tdl.com/~wako/

Canyon Directly Downstream of Lake Almanor Dam.

This is a brief stop to look at Quaternary basalts exposed in the walls of the narrow canyon directly downstream from Lake Almanor dam. The best viewing of this exposure is from the east side of the outlet of the dam. The cliffs on the west side of the canyon are made up of the 400 ka Basalt of Westwood overlying the 600 ka Basalt of Warner Valley. The base of the Basalt of Westwood is seen as

a degraded (less massive) zone possibly including an old soil, that overlies more massive basalt of the Basalt of Warner Valley. Argon-argon samples were collected from the cliff you are viewing; these samples verified the presence of the two flow units. From where we park our vehicles we can see a topographic step (facing us) on the west side of the river. This is the scarp of the Skinner Flat fault in Basalt of Westwood. The scarp is up to 10 m high and also bounds the southwest (uphill) side of the area that we will camp. In addition to the scarp, the surface of the Basalt of Westwood slopes northeastward toward the lake. Because this is the upstream direction, this slope is most likely of tectonic origin.

References (STOPS 7 & 8)

Muffler, L.J.P., Clynne, M.A., and Champion, D.E., 1994, Late Quaternary normal faulting of the Hat Creek basalt, northern California: Geological Society of America Bulletin, v. 106, p. 195-200.

Page, W. D., Sawyer, T. S., McLaren, M. , Savage, W. U., and Wakabayashi, J., 1993, The Quaternary Tahoe-Medicine Lake trough: the western margin of the Basin and Range transition, NE California: Geol. Soc. Amer. , Abstr. w. Programs, v. 25, no. 5, p. 131.

Wakabayashi, J., and Sawyer, T.L., 2001, Stream incision, tectonics, uplift, and evolution of topography of the Sierra Nevada, California: Journal of Geology, v. 109, p. 539-562.

Wakabayashi, J., and Sawyer, T.L., 2000, Neotectonics of the Sierra Nevada and the Sierra Nevada-Basin and Range Transition, California, with field trip stop descriptions for the northeastern Sierra Nevada: in Brooks, E.R., and Dida, L.T., eds., Field guide to the geology and tectonics of the northern Sierra Nevada, California Division of Mines and Geology Special Publication 122, p. 173-212.

Wills, C. J., 1990, Active faults north of Lassen Volcanic National Park, northern California: California Geology, v. 44, p. 51-58.

WLA (William Lettis and Associates), 1996, Lake Almanor and Butt Valley Dams Seismic Stability Assessment, Volume 1: Seismic Source Characterization and Estimated Ground Motions: report to Pacific Gas and Electric Company.

STOP 9

Thomas L. Sawyer[1] and Rich Briggs[2]
[1]*Piedmont Geosciences, Inc., 10235 Blackhawk Drive, Reno, NV 89506, Piedmont@USA.com*
[2]*University of Nevada Reno, Center for Neotectonic Studies, Reno, NV 89557, briggs@seismo.unr.edu*

with prior contributions by:
Mark A. Hemphill-Haley[3] and William D. Page[4]
[3]Geosciences Dept., PG&E, P.O. Box 770000, San Francisco, CA 94177
[4]Geology Dept., Humboldt State University, Arcata, CA 95521

Kinematics and late Quaternary activity of the Mohawk Valley Fault Zone

Objective

The main purpose of this stop is to discuss the late Quaternary activity of the Mohawk Valley fault zone (MVFZ) based on geomorphic and trenching studies, as well as discuss the possible significance the fault zone may have in accommodate northwest-directed right-lateral shear measured geodetically across the northern Walker Lane. In addition, our vantage point above the town of Clio in Mohawk Valley provides a general overview of the geomorphology of the eastern front of the Sierra Nevada, topography produced by late Pliocene to late Quaternary movement on the MVFZ.

Overview

The MVFZ is the frontal fault of the Sierra Nevada from south of Sierra Valley northwest to American Valley, a distance of 60 km or more. In addition to forming the present topography along this part of the northern Sierran front, the MVFZ is optimally oriented to accommodate northwest-directed right shear along the western edge of the Basin and Range/Sierra Nevada transition in the northern Walker Lane. In addition, the fault zone is expressed as the "Plumas Trough" of Durrell (1966), which is one in a series of en echelon late Neogene graben that extend from the Tahoe basin to the Medicine Lake volcanic field (Page et al., 1993) and probably another 100 km northward to the Klamath Lake region of Oregon, or beyond.

Recently, Henry and Perkins (2001) suggested that the uplift of the Sierra Nevada relative to the Basin and Range began at 3 Ma in the Reno area, based on structural analysis of the Verdi-Boca sedimentary basin and 40Ar/39Ar dating and tephrochronology of volcanic units underlying, within, and overlying sediment in the basin. Henry and Perkins (2001) reported that the results of their study are consistent with apatite-fission-track and U-Th/He results that show uplift of the Carson Range, also within the northern Basin and Range/Sierra Nevada transition, at 3 Ma (Surpless et al., 2000). However, northwest-directed right shear began after 3 Ma in the Reno area or was accommodated to the east (Henry and Perkins, 2001).

Considering that the fault zone is less than 30 km from the Carson Range and sedimentary remnants of the dismembered and formerly extensive Verdi-Boca basin presently lie less than 25 km south along the Sierran front (Henry and Perkins, 2001), movement on the MVFZ also may have began at 3 Ma and perhaps right-lateral shear began somewhat latter.

The MVFZ is one of the more seismically active frontal faults of the Sierra Nevada (Gotter et al., 1994). In addition to abundant microseismicity, nine earthquakes of M=4 or larger have occurred along or near the MVFZ since 1974 (USGS-NEIC Internet resource, 2001). The largest and most recent of these events, a M=5.5 earthquake on August 10, 2001, occurred near the north end of Mohawk Valley 17 km beneath the west flank of Grizzly Ridge. This event, which proceeded a M=4.2 event on the following day, has a focal mechanism that is consistent with right-lateral slip on a northwest-striking nodal plane parallel to the MVFZ. The largest historical earthquake reported in the region was a moderate earthquake (M~6) that occurred in April, 1888. This earthquake reportedly was associated with ground cracking in Mohawk Valley near Clio. However, Toppozzada and others (1981) re-evaluated the felt reports of this event and concluded that the earthquake likely occurred in the Honey Lake region.

Geodesy along the northern Basin and Range/Sierra Nevada transition

Kinematic models and geodetic studies have shown that 20-25% of the relative motion between the Pacific and North American plates occurs east of the Sierra Nevada at the latitude of the northern Walker Lane (Atwater, 1970; Minster and Jordan, 1987; DeMets et al. 1987; Ward, 1990; Argus and Gordon, 1991; Dixon et al., 1995). Recent GPS geodetic studies across the northern Basin and Range (the continuous BARGEN (Bennett et al., 1998) and campaign USGS (Thatcher et al., 1999) networks) and within the Sierra Nevada (Dixon et al., 2000) have significantly increased the resolution of strain data along the northern Basin and Range/Sierra Nevada transition. These studies demonstrate that the bulk of strain accumulation in the northern Basin and Range occurs between the Sierra Nevada and the Central Nevada Seismic Belt (CNSB) (Fig. 9-2), and that the Sierra Nevada effectively acts as a microplate with little internal deformation. From east to west, velocity vectors across the northern Basin and Range generally increase in magnitude and rotate from east-west orientations to northwest directions with respect to stable North America, reflecting a transition from primarily extension in the east to increasing northwest-directed, right-lateral shear near the Sierra Nevada (Fig. 1; BARGEN vectors only for clarity). While the big picture is in place, however, details of how strain is distributed with respect to active faults along the northern Basin and Range/Sierra Nevada transition are not yet clear.

Existence, persistence, and magnitude of the strain gradient associated with the northern Walker Lane

A significant velocity gradient, or suddenly increased strain rate, appears to be associated with the northern Walker Lane. USGS stations along the Highway 50 corridor show increase in station velocities corresponding to the Walker Lane (Fig. 9-2) (Thatcher et al., 1999). BARGEN stations aligned with the USGS transect (stations NEWP, UPSA, SLID) also show a subdued, but a detectable increase in station velocities near the southern edge of the northern Walker Lane. In contrast, BARGEN station velocities farther north (LEWI, TUNG, GARL, SHIN, QUIN) do not show a significant jump in velocities, but instead reflect more evenly distributed strain. Velocity differences between BARGEN stations UPSA or GARL and SLID in the south (5-6mm/yr) are large when compared to SHIN and QUIN in the north (2-3mm/yr) (Fig. 9-2), implying that strain becomes more broadly distributed to the north. Bennett and others (1999) interpret only 2-3 mm/yr of right-lateral shear remaining at 41^{o}, with the bulk of deformation transferred northeastward into Basin and Range extension. This is consistent with prior observations and kinematic models of the transition from strike-slip faulting in Mohawk Valley to extension in northeastern California and Oregon (Grose, 1986; Pezzopane and Weldon, 1993; Unruh, 1996).

Geodetic context of the Mohawk Valley fault zone

The MVFZ is optimally oriented to accommodate the northwest-directed deformation measured geodetically across the northern Walker Lane. Preliminary measurements of relative velocities across the northern Walker Lane appear to show a transition from 4-8 mm/yr at its southern extent to 2-3 mm/yr near Quincy. Fault slip rate estimates for the region do not presently account for this strain accumulation (Briggs and Wesnousky, 2001). With the exception of the Honey Lake fault zone (~2 mm/year; Wills and Borchardt, 1993), slip rates have not been determined geologically for active strike-slip faults in this portion of the Basin and Range/Sierra Nevada transition. It is likely, based on previous geomorphic and trenching work (Sawyer et al., 1993), that the MVFZ takes up a significant portion of the geodetically measured dextral shear at its latitude.

A first-order attempt to model the amount of slip taken up by the MVFZ based primarily on geodetic measurements has been pursued by Dixon and others (2000) (Fig. 9-3). A simple elastic half space is used to model only two faults, the Honey Lake fault slipping at 2 mm/yr (Wills and Borchardt, 1993) and the MVFZ. Boundary conditions are the stable Sierran microplate translating to the northwest at nearly 14 mm/yr to the west and near-zero velocity (fixed) to the east. This model yields slip of 6□3 mm/yr on the MVFZ. Preliminary geologic work (Sawyer et al., 1993) indicates that a slip rate near or below the lowest limit (3 mm/yr) is most likely.

While the simple model of Dixon and others (2000) appears to overstate the slip rate on the MVFZ, it does highlight the potential for this fault to accommodate significant slip in this region. Increased geologic and geodetic information across the northern Walker Lane will be required if more realistic slip models are to be formulated. A campaign network of 16 GPS stations extending across this region has been in place since June 2000, and results will hopefully clarify strain distribution across the northern Walker Lane (Briggs and Wesnousky, 2001) (Fig. 9-4). Geodesy alone will provide only a rough sketch of strain accumulation across the region, however, and geologic and paleoseismic study of active northern Walker Lane faults will be necessary to understand how regional strain is released by earthquakes. This effort is underway - in addition to this investigation of the MVFZ, similar studies are ongoing on the Warm Springs fault zone (Craig dePolo and others), the Peavine fault (Alan Ramelli and others), and the Olinghouse and Pyramid Lake faults (Rich Briggs and Steve Wesnousky).

Mohawk Valley Fault Zone

The MVFZ is the frontal fault of the Sierra Nevada from south of Sierra Valley northwest to American Valley. However the steep, prominent Sierran front only extends along the western edge of southern Sierra Valley and of southern Mohawk Valley, where it is particular linear and relatively undissected. Paralleling the frontal fault or western branch of the southern MVFZ is an eastern branch that crosses the floor of Sierra Valley, between Sierraville and Calpine, and traverses the volcanic and granitic hills between Sierra and Mohawk valleys (Figure 9-1). The eastern branch appears to extend northwest along the east side of Mohawk Valley and American Valley and may account for most or all late Quaternary slip on the northern MVFZ. The character of the Sierran front changes near the town of Clio, apparently reflecting decreased activity on the western branch and a transfer of right slip across southern Mohawk Valley to the eastern branch in a releasing right stepover. Northwest from Clio, the front of the range is less steep and more dissected, and the western branch is concealed by massive landslide deposits and, further northwest, by unfaulted late Pleistocene lateral moraines and glacial till (Hawkins et al., 1986; Saucedo, 1992).

The parallel branches of the MVFZ are 3 km apart (Figure 9-1) and have contrasting geomorphic expressions and different styles of faulting. The western branch, first mapped by Turner (1897), downfaults the Miocene to middle Pliocene Mehrten Formation 500 to 700 m from the crest of the Sierra Nevada to the Mehrten capped hills between Mohawk and Sierra valleys (Turner, 1897; Sawyer et al., 1993) and 20 km to the northwest downfaults both the stratigraphically higher Mehrten Formation and the 16 Ma Lovejoy Basalt an estimated 1,200 m (Page and Sawyer, 1992) into the semi-rhombic depression at the town of Sloat. Whereas, the eastern branch is marked by a series of linear northwest-striking scarplets, deflected and ponded drainages, and tonal and vegetation lineaments crossing the floor of southern Sierra Valley, that were first mapped by Sawyer et al. (1993). In addition, the eastern branch lacks range-front relief and the more continuous fault traces display a left en echelon arrangement. The pattern of faulting and the contrasting geomorphic expression of the two branches are generally similar to that of the Owens Valley and Independence faults, respectively. Thus, as in the Owens Valley area, strain partitioning apparently occurs along the southern MVFZ.

Applying this late Neogene displacement data and assuming that vertical movement on the fault zone began at 3 Ma, a maximum long-term average, vertical slip rate of 0.2 mm/yr would characterize the western branch along the southern MVFZ and a rate of 0.4 mm/yr would characterize it along the central MVFZ.

Historical seismicity, recent geodetic data, and the pattern and geomorphic expression of faults in the zone, however, suggest that in addition to vertical displacement, the MVFZ accommodates a possibly significant component of right-lateral slip in the northern Walker Lane. Right-lateral strike-slip faulting is consistent with results of our paleoseismic study as well, which was conducted at the toe of the Sierran Front between Mohawk Valley and Sierra Valley and west of the town of Calpine (Figure 9-1).

Although uncharacterized, the cumulative amount of right slip on the MVFZ may be substantial. For example, the Middle Fork Feather River abruptly jogs northwest at Clio and does not resume its westerly course until near the town of Cromberg, possibly reflecting a 18 to 20 km right-lateral deflection

and/or offset along the northern MVFZ. The unique aspect of the Feather River as being the only drainage system to flow across the entire width of the Sierra Nevada may reflect an antecedent drainage condition, which would tend to support the inference that the drainage has been laterally offset.

Assuming that the Middle Fork Feather River is offset 18 to 20 km along the MVFZ and, further that strike-slip faulting began at 3 Ma or latter in the Mohawk Valley area, then a maximum right-lateral slip rate of 6-7 mm/yr is permissive, albeit unlikely, on the MVFZ. It is interesting to note that this rate is comparable to results of kinematic models and geodetic studies. Further study and additional information will be required to constrain the rate of slip on the MVFZ.

Paleoseismic investigation of the MVFZ at the Calpine trench site

Alt (1990) identified a site for paleoseismic investigation along the west branch of the southern MVFZ, 4 km west of Calpine, based on interpretation of aerial photographs and aerial reconnaissance. The "Calpine trench site" is at the abrupt toe of the steep and high Sierran front at 5,800 ft in a dense conifer forest. The initial trenching target was a distinct range-front graben. An additional trench was sited across a steep well-defined scarp on colluvium identified along a sympathetic fault splaying from the frontal fault (Figure 9-1).

Two exploratory trenches were excavated in December, 1990 at the Calpine trench site. Trench 1 was excavated within the range-front graben and crossed an antithetic fault. Trench 2 crossed a 3.7-m-high, northeast-facing scarp marking the arcuate splay fault (Figure 9-1). The prominent scarp trends N67ºW at the trench, slightly oblique to the N50ºW-trend of the nearby range front. As a result of inclemental weather, however, shallow groundwater seeping from small pores in the trench walls immediately froze forming 2-3 inch long needles of ice that completely obscured the walls of the trenches and forced us to postpone the trench study. In August, 1991, we re-excavated and logged the eastern part of trench 1, which exposed the antithetic fault, and re-excavated and logged all of trench 2.

Trench 1 Findings: Trench 1 was approximately 60 m long and up to 3 m deep. The trench exposed coarse colluvium interfingering eastward with flat-lying, fine-grained alluvial deposits near the axis of the graben. The alluvial deposits interfingered eastward with another package of colluvial deposits. A fragment of charcoal from near the base of unit C1, the uppermost deposit in this package, yielded a radiocarbon date of 3,395 + 105 ^{14}C yr BP. A second charcoal fragment was collected from an irregular shaped and bioturbated deposit that infilled above a burned tree stump in growth position. This sample yielded a date of 4,735 + 155 ^{14}C yr. BP.

A common problem in attempting to date near-surface deposits in a dense forest setting is the introduction of secondary or intrusive organic matter as a result of extensive bioturbation. Radiocarbon dates on intrusive charcoal postdate the age of the host deposits and may best explain the stratigraphic inversion problem of the two dates from trench 1. Therefore, unit C1 most likely is not younger than middle Holocene in age (Figure 9-5).

Although the range front fault was not exposed, it presumably lies further to the west and higher on the range front, trench 1 did expose the antithetic fault bounding the east side of the range-front graben. Two steeply west-dipping faults in a 4-m-wide zone of near-vertical fractures were exposed cutting and juxtaposing colluvial deposits (Figure 9-5). The eastern of the two faults, F1, is marked by a 25-cm-wide zone of prominent shear fabric that strikes N40º-45^{O}W and dips from 34^{O}-81^{O}W. The fault truncates upwards at the base of colluvial unit C2, which is overlain by the middle(?) Holocene unit C1. The cumulative stratigraphic separation across fault F1 probably exceeds 2 m, down to the southwest. The western fault, F2, was identified as a 10-cm-wide zone of shears and fractures that strikes N25^{O}W and steepens downward from 52^{O}W near the top of the trench to 72^{O}W near the bottom. The expression of this fault diminishes towards the surface, but can be identified to where it also truncates against the base of unit C2 (Figure 9-5). Stratigraphic separation across fault F2 exceeds 2 m.

The zone of steeply-dipping fractures is confined to the footwall of the fault F1 (Figure 9-5). The fractures generally strike N65^{O}W and dip from 75^{O}W through vertical to approximately 87ºE. Roots and

root mats commonly occur along, and aid in identification of, these fractures. The fracture zone cuts units C6 and C7 and truncates at the base of unit C5 (Figure 9-5).

Trench 2 Findings: Trench 2 was nearly 50 m long, up to 5.5 m deep, and exposed colluvial deposits, including scarp-derived colluvium, overlying and juxtaposed against weathered granitic bedrock. From youngest to oldest, the colluvial deposits are designated C1 through C8 and Cw1 through Cw5 (Figure 9-6). Bedrock was encountered in the footwall of the splay fault.

Two samples of charcoal collected from the youngest colluvial deposit, unit C1, yielded radiocarbon dates of 3,055 + 130 ^{14}C yr BP and 12,081 + 94 ^{14}C yr BP (Figure 9-6). Two additional samples of charcoal collected from the subjacent colluvial unit, C2, yielded dates of 1,032 ± 50 to 3,360 ± 56 ^{14}C yr BP (Figure 9-6). The spread and stratigraphic inversion of these dates likely results from the introduction of secondary charcoal by bioturbation. Although these deposits may be Holocene in age, units C1 and C2 are likely latest Pleistocene in age given the apparent problem with intrusive organic matter.

Trench 2 exposed a rather wide zone of steeply- to near-vertical faults and fractures. The main fault, F1, juxtaposes granitic bedrock and colluvial deposits in the footwall against colluvial deposits in the hanging wall. The upper extent of the fault bounds a fissure-fill deposits, unit FF2 (Figure 9-6). The fault strikes N72^{o}W, slightly oblique to the local trend of the scarp, and dips 57^{o}E. The fault exhibits distinct shear fabric and near vertically aligned clasts within a shear zone up to 60 cm wide. The vertical separation across fault F1 exceeds 3.9 to 4.4 m. Slickenside striations plunge a modest 15^{o}SE, suggesting dominantly right-lateral slip with a subordinate normal component on the range-front splay fault. The stratigraphic separation across fault F1 and these shear-sense indicators suggest that fault F1 may have produced 15 to 17 m of right-lateral displacement in the late Quaternary.

Trench 2 exposed three additional and subordinate faults, F2, F3 and F4 (Figure 9-6). Fault F2 is oriented N53^{o}W55^{o}E and exhibits only minor stratigraphic offset. This fault extends upwards to the base of unit C3 as a single fracture. Fault F3 strikes N51^{o}W, dips 85^{o}E, and also truncates upwards at the base of C3. This fault juxtaposes bedrock against colluvium in an apparent reverse sense, indicating lateral slip also occurs on fault F3. The down-to-the-east offset of the top of bedrock across fault F3 is estimated to be about 3.8 meters. Fault F4 is oriented N31^{o}W85^{o}E and offsets of the top of bedrock about 50 cm. This fault is associated with numerous fractures, an infilled fissure, and a small "colluvial-wedge" deposit, unit Cw3.

In addition, several high-angle fractures were exposed in trench 1. Most of these fractures are planar and strike N51º to 77^{o}W and dip steeply to the east. However, a few fractures are slightly arcuate and some dip westward. Although none of the faults were found to cut deposits younger than unit C4, three distinct fractures cut through the lower two-third's of overlying unit C2.

Paleoseismic Interpretation: Our interpretation of 6 to 7 earthquakes during the late Quaternary along the western branch of the MVFZ is based on the upward termination of faults and fractures, fissure-fill deposits, scarp-derived colluvium, the relative degree of clast weathering and soil development, and radiocarbon dates in trench 2 (Figure 9-7). Some or all of the events interpreted from trench 1 exposures may be represented in the other trench.

The first of a minimum of four surface-faulting events, "earthquake X", interpreted from trench 1 exposures of the antithetic fault (Figure 9-7) is evidenced by a set of fractures that disrupt units C6 and C7, but are abruptly truncated at the base of unit C5 (Figure 9-5). The second event, earthquake V, is interpreted to have separated units C5 through C7 a minimum of about 180 cm, down to the west, along fault F1. Unit Cw2 is thought to be a colluvial wedge derived from, and deposited against a scarp produced during this event. The penultimate event (earthquake U) faulted unit Cw2 along fault F2, and is associated with a comparable amount of vertical separation and with scarp-derived colluvial . The colluvial wedge resulting from the penultimate earthquake, unit Cw1, is buried by units C2 through C1a which likely provide a minimum time since the occurrence of the penultimate event of at least 5 ka . The

fourth, and most-recent event (earthquake T?, Figure 9-7), is inferred from youthful scarps and small closed depressions, that were first noted by Craig M. dePolo as extending northward along strike of the antithetic fault from trench 1. Evidence for this event was not recognized in the trench, presumably because it was obliterated by bioturbation in the fault zone.

The earliest of 6 to 7 events interpreted from trench 2 exposures, earthquake Z (Figure 9-7), produced a bedrock scarp along fault F3. Unit Cw5 is a colluvial wedge (Figure 9-6) derived from weathered bedrock exposed in the footwall of the fault during the event. The second event, earthquake Y, re-ruptured fault F3 and may have triggered minor slip along fault F2. Unit Cw4 is a colluvial wedge deposited at the base of the second-event scarp. The estimated thickness of Cw4 against the fault suggests that the second event resulted in at least 2.6 m of vertical displacement on a fault having an inferred lateral slip component. Earthquake X is the third paleoseismic event interpreted from trench 2 exposures and it produced a scarp in weathered bedrock along fault F4, buried by colluvial-wedge Cw3. The fourth event, earthquake W, is inferred from stratigraphic relationships along fault F1. Unit Cw2 is a colluvial wedge deposit derived from a scarp produced during this event. The thickness of the scarp-derived colluvium suggests that this event produced 1.3 m, or more, of down-to-the-east normal slip on fault F1, which based on the orientation of slickensides has a significant component of lateral slip. The fifth event, earthquake V, is interpreted from fissure-fill deposit FF2, which is in fault contact with hanging wall units Cw2 and C5. The penultimate event, earthquake U, produced a scarp buried by unit Cw1. Fracturing in the lower two-third's of unit C2 is the only evidence in trench 2 for the most recent event.

This paleoseismic investigation suggests that rupture along the western branch of the southern MVFZ occurs during large earthquakes, that are possibly characterized by right-oblique-normal displacements in excess of 2-3 m.

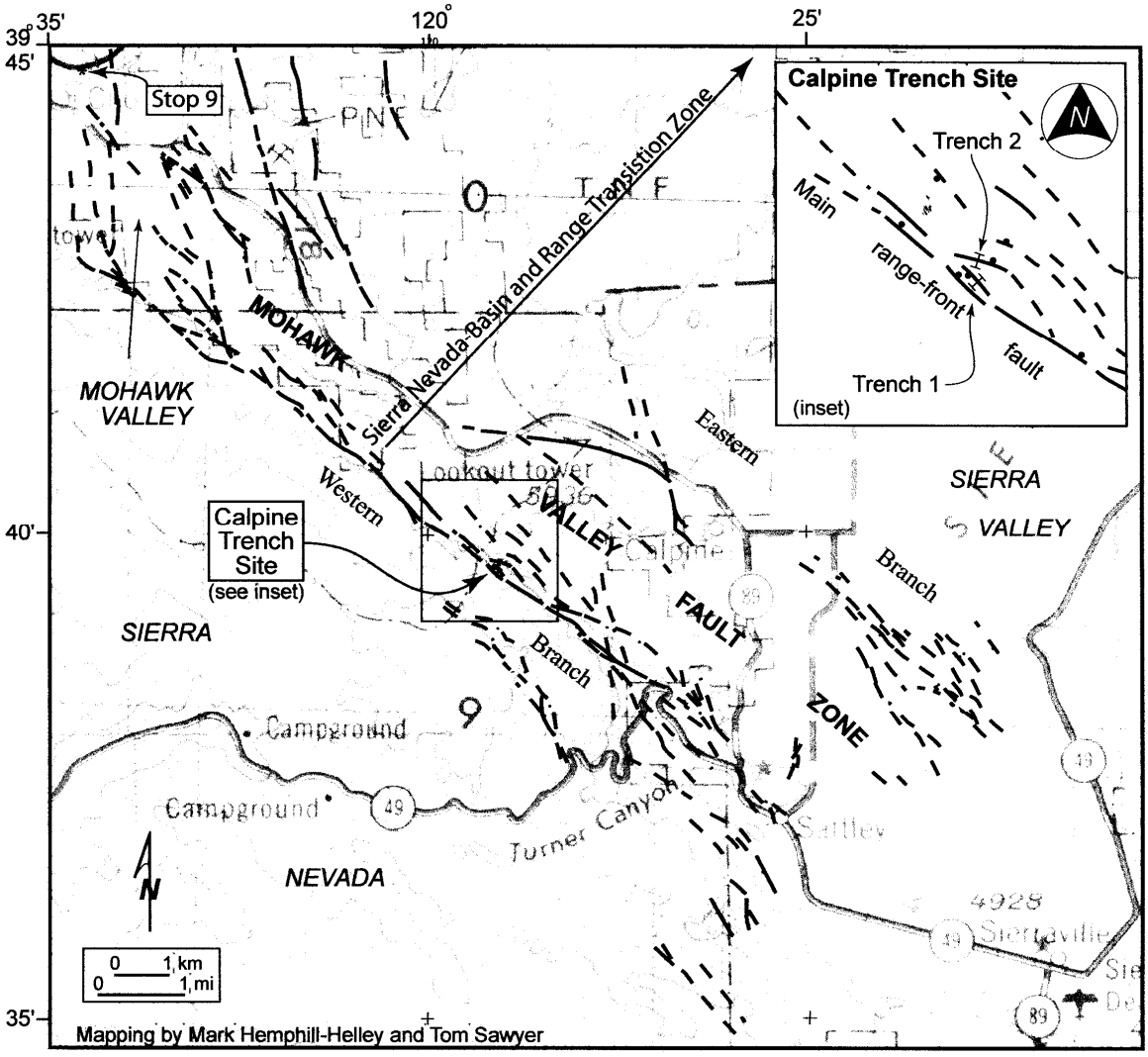

Figure 9-1. Map of the southern Mohawk Valley fault zone, based on interpretation of aerial photographs and limited field reconnainance.

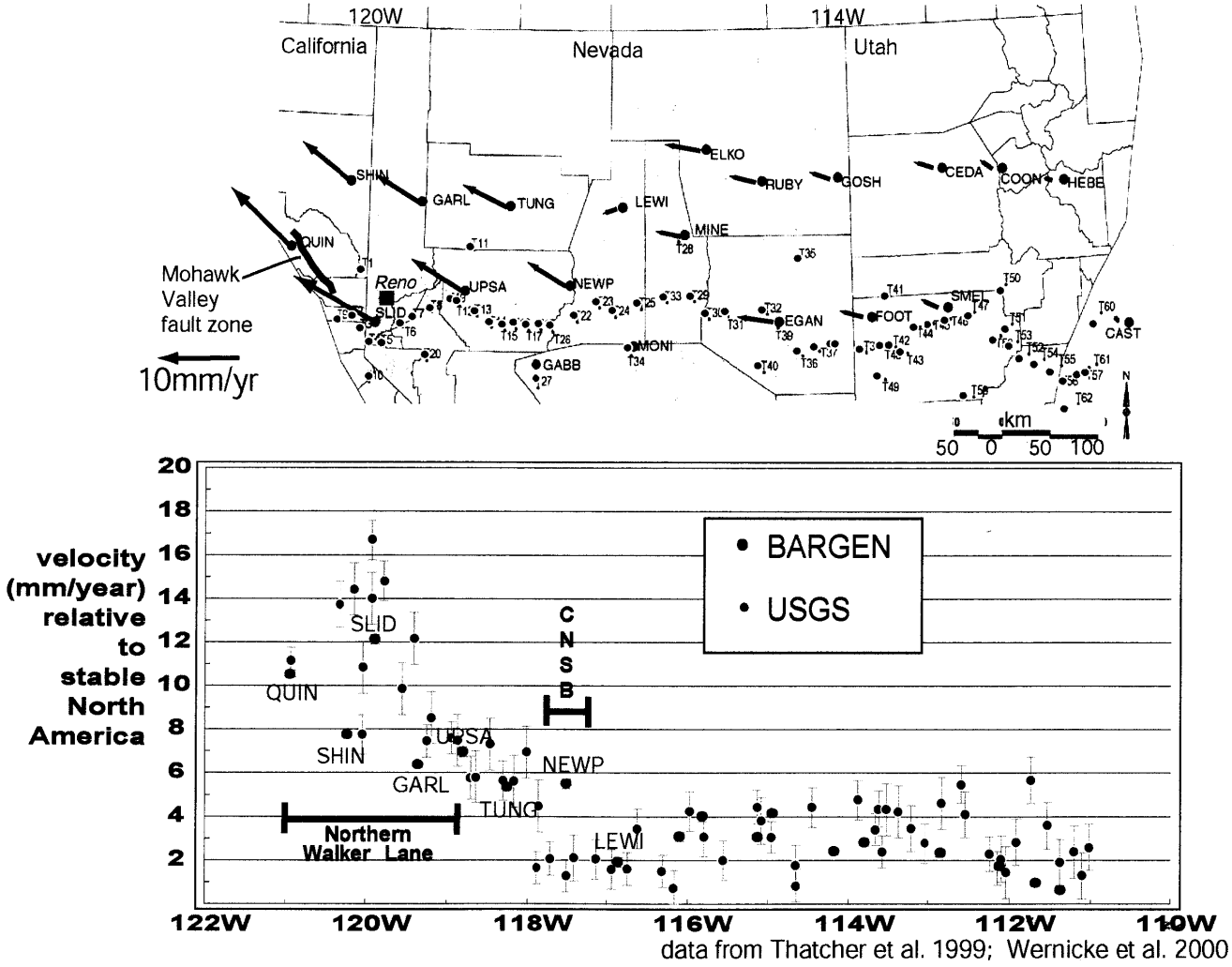

Figure 9-2. USGS and BARGEN geodetic networks. The top panel shows station locations for both networks and velocity vectors for the BARGEN network. The bottom panel shows absolute station velocities for both networks relative to stable North America. Note shared station QUIN.

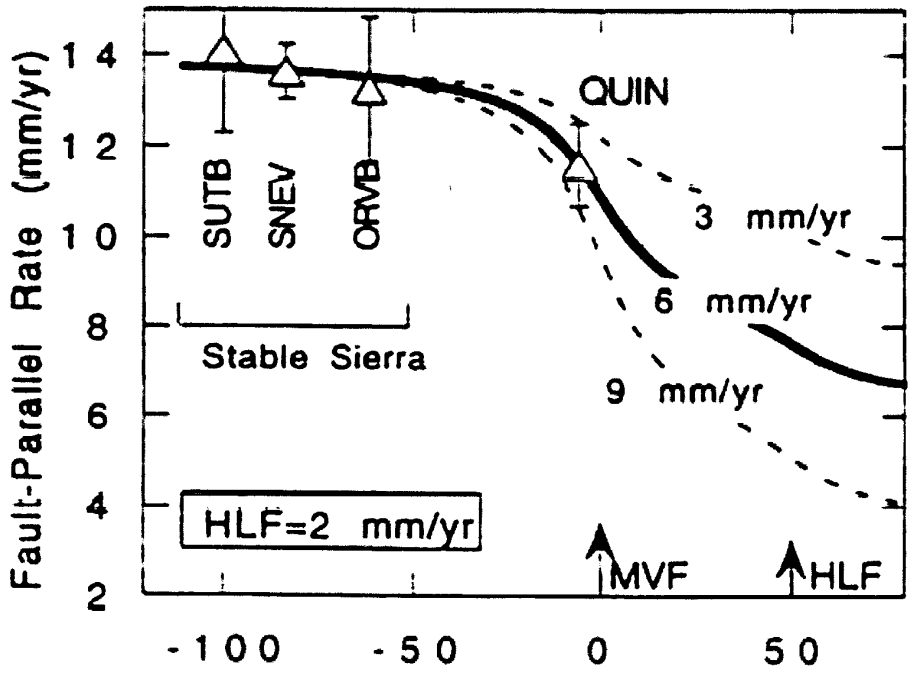

Figure 9-3. Simple strain accumulation model for two strike-slip faults in an elastic half-space (figure from Dixon et al., 2000). MVF = Mohawk Valley fault zone, HLF = Honey Lake fault zone. Honey Lake fault zone is fixed at 2mm/yr (Wills and Borchardt, 1993).

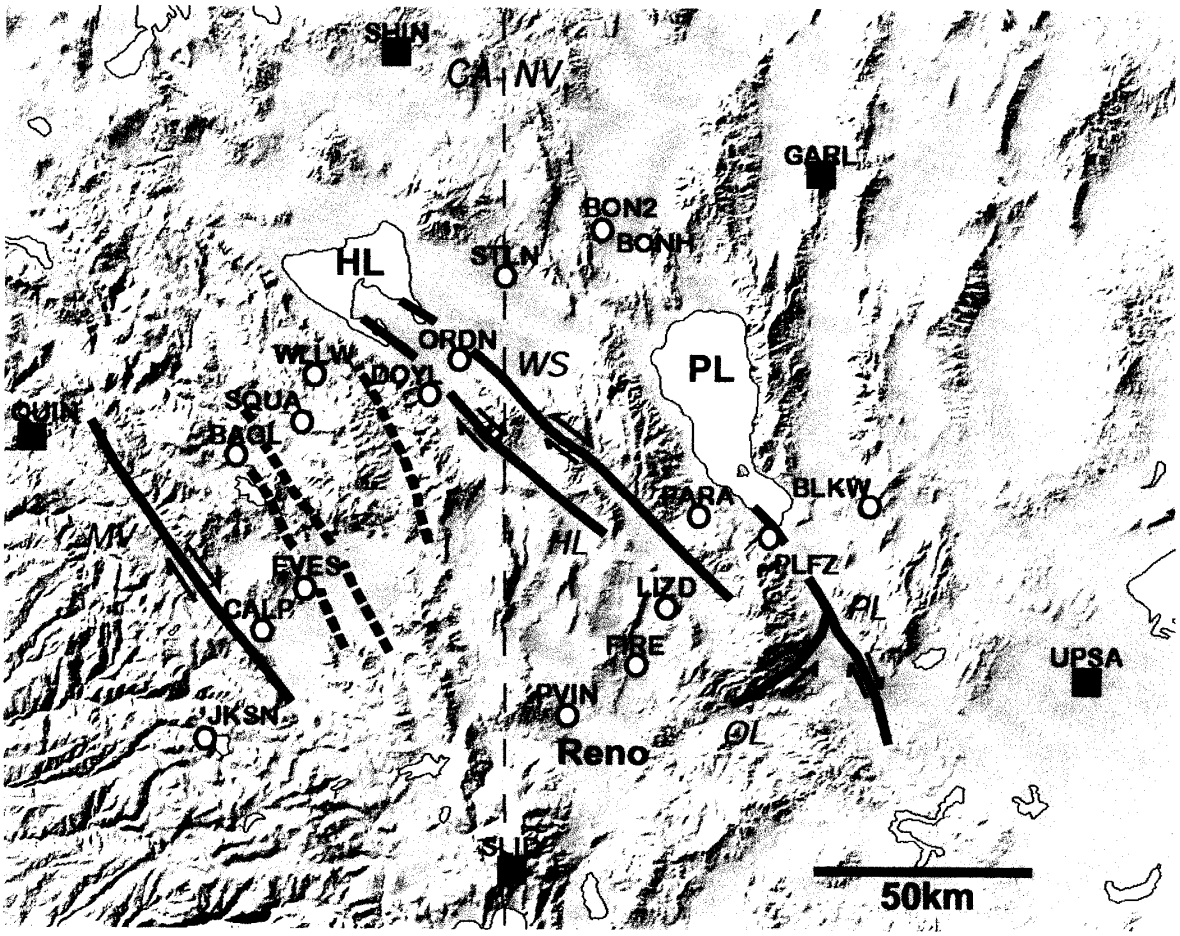

Figure 9-4. Circles denote stations of the Northern Walker Lane Geodetic Network. Existing continuous BARGEN (Bennett et al., 1998) stations are shown as squares. Major strike-slip faults are shown by solid lines (MV=Mohawk Valley; HL=Honey Lake; WS=Warm Springs; PL=Pyramid Lake; OL=Olinghouse).

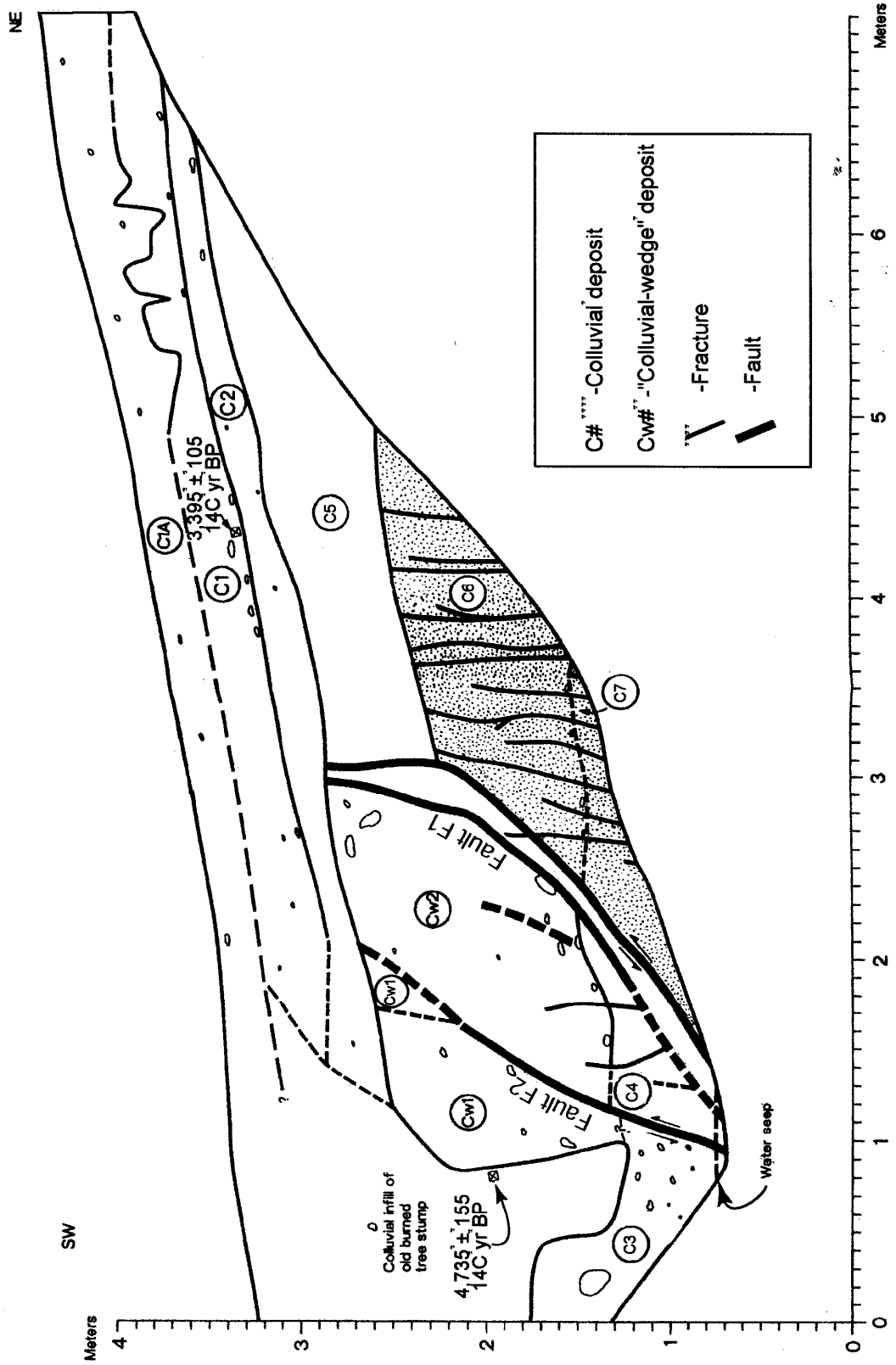

Figure 9-5. Graphical log of eastern part of Trench 1, Calpine trench site.

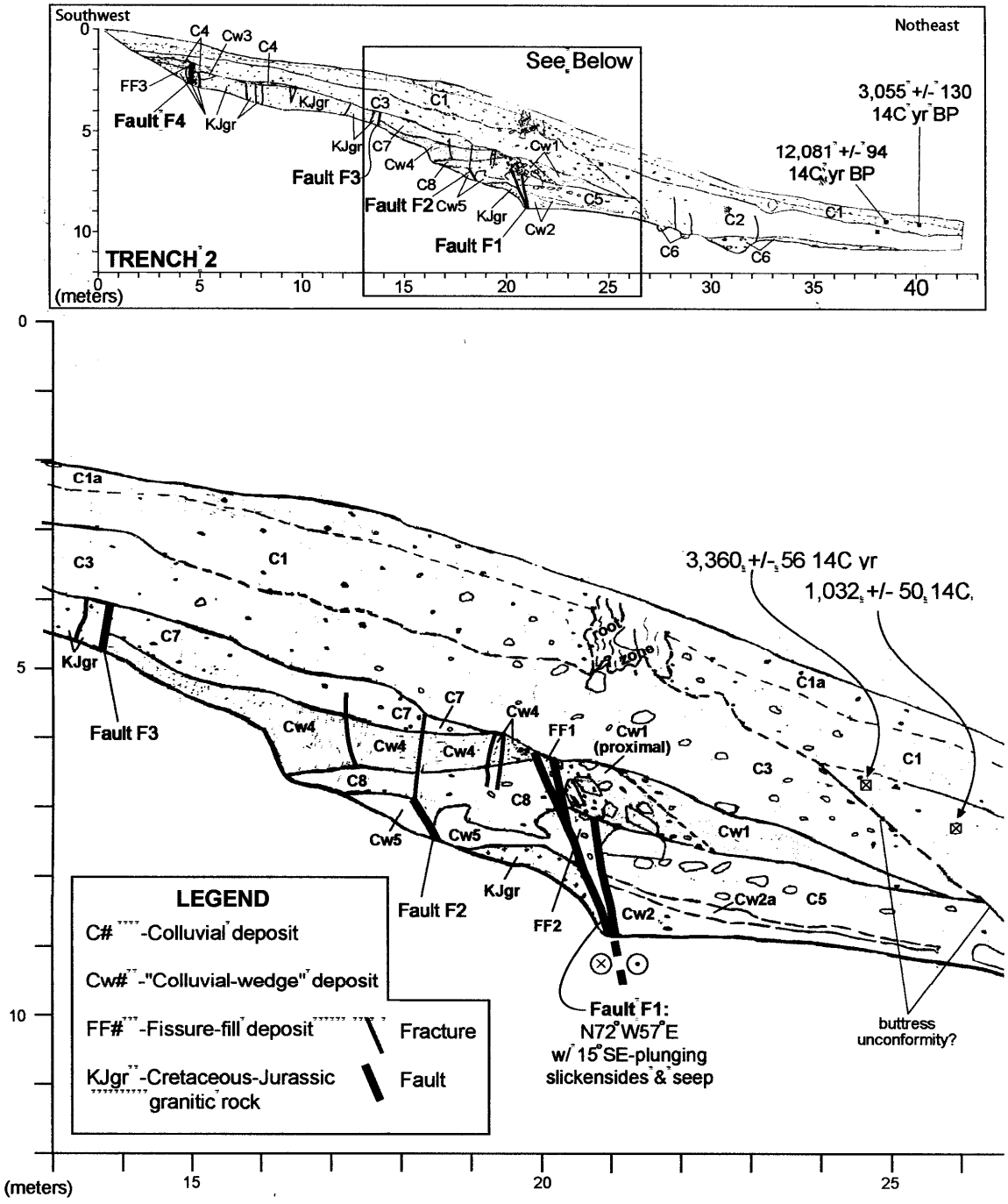

Figure 9-6. Graphical log of north wall of Trench 2, Calipine trench site.

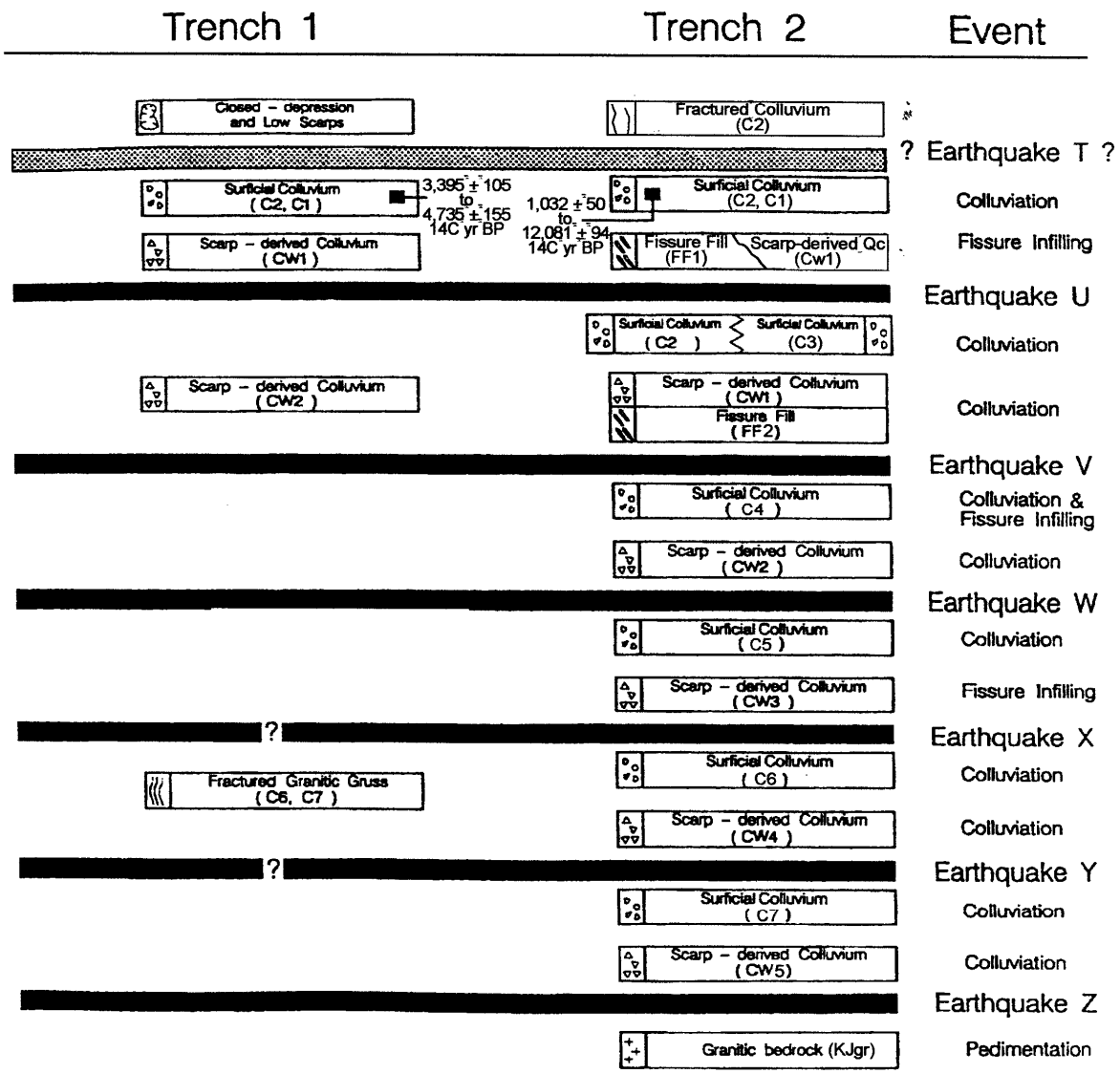

Figure 9-7. Relative chronology of paleoseismic surface-faulting events at the Calpine trench site.

References

Alt, J.N., 1990, Observations and Preliminary Conclusions from Mohawk Study, unpublished consultants report to PG&E, Geosciences Department, San Francisco, Ca, 2 p. with plates.

Argus, D.F., and R.G. Gordon, 1991. Current Sierra Nevada-North America motion from very long baseline interferometry; implications for the kinematics of the Western United States. Geology, vol.19, no.11, pp.1085-1088.

Atwater, T., 1970. Implications of Plate Tectonics for the Cenozoic Tectonic Evolution of Western North America. GSA Bulletin, v. 81, pp 3513-3536.

Bennett, R.A., B.P. Wernicke, and J.L. Davis, 1998. Continuous GPS measurements of contemporary deformation across the northern Basin and Range province. Geophys. Res. Letters 25:4, pp 563-566.
Bennett, R.A., Wernicke, B.P., Davis, J.L., Friedrich, A., and Niemi, N.A., 1999. Distribution of extension and shear across the northern Basin and Range from BARGEN continuous GPS data: The fate of the eastern California shear zone. Eos, Transactions, American Geophysical Union, vol.80, no.46, pp. F269.
Briggs, R.W. and S.G. Wesnousky, 2001. The Basin and Range Sierra Nevada Transition along the Northern Walker Lane: Geology vs. Geodesy. Seismological Research Letters, v.72, no.2, p.280.
DeMets, C., Gordon, R.G., Stein, S., and Argus, D.F., 1987. A revised estimate of Pacific-North America motion and implications for western North America plate boundary zone tectonics. Geophysical Research Letters, vol.14, no.9, pp.911-914.
Dixon, T. H., S. Robaudo, J. Lee, and M.C. Reheis, 1995. Constraints on present-day Basin and Range deformation from space geodesy. Tectonics 14:4, pp 755-772.
Dixon, T.H, M. Miller, F. Farina, H. Wang, and D Johnson, 2000. Present-day motion of the Sierra Nevada block and some tectonic implications for the Basin and Range province, North American Cordillera. Tectonics 19:1, pp. 1-24.
Durrell, C., 1966, Tertiary and Quaternary geology of the northern Sierra Nevada, in E.H. Bailey, editor, Geology of Northern California: California Division of Mines and Geology Bulletin 190, pp. 185-197.
Gotter, S.K. Oppenheimer, D.H., Mori, J.J., Savage, M.K., Masse, R.P., 1994, Earthquakes in California and Nevada: U.S. Geological Survey Open-File Report 94-647, scale 1:1,000,000.
Grose, T.L.T., 1986, Geologic map, Marlette Lake quadrangle: Nevada Bureau of Mines and Geology Map 2Cg, 1:24,000.
Grose, T.L.T., 1996. Tectonics of the Walker Lane in NE California and the Honey Lake anomaly. Eos, Transactions, American Geophysical Union, vol.67, no.44, pp.1211.
Hawkins, F.F., LaForge, R., and Hansen, R.A., 1986, Seismotectonic study of the Stampede, Prosser Creek, Boca, and Lake Tahoe dams, Truckee/Lake Tahoe area, northeastern Sierra Nevada, California: Seismotectonic Report No. 85-4, 210 p.
Henry, C.D. and Perkins, M.E., 2001, Sierra Nevada-Basin and Range transition near Reno, Nevada: Two-stage Development at at 12 and 3 Ma: Geology, v. 29, no. 8, p. 719-722.
Minster, J.B. and T.H. Jordan, 1987. Vector constraints on Western U.S. deformation from space geodesy, neotectonics, and plate motions. Journal of Geophysical Research, B, Solid Earth and Planets, vol.92, no.6, pp.4798-4804.
Page, W.D. and Sawyer, T.L., 1992, Tectonic deformation of the Lovejoy basalt, a late Cenozoic strain guage across the northern Sierra Nevada, California EOS v. 73, p 590.
Page, W.D., Sawyer, T.L., McLaren, M., Savage, W.U., and Wakabayashi, J., 1993, The Quaternary Tahoe-Medicine Lake trough: the western margin of the Basin and Range transition, NE California: Geological Society of America, Abstracts with programs, v. 25, p. 131.
Pezzopane, S.K. and R.J. Weldon, 1993. Tectonic role of active faulting in central Oregon. Tectonics, vol.12, no.5, pp.1140-1169.
Saucedo, G.J., 1992, Geologic map of the Chico quadrangle, California: California Division of Mines and Geology, scale 1:250,000
Sawyer, T.L., Page, W.D., and Hemphill-Haley, M.A., 1993, Recurrent late Quaternary surface faulting along the southern Mohawk Valley fault zone, NE California: Geological Society of America, Abstracts with Programs, v. 25, p. 142.
Surpless, B.E., Stockli, D.F., Dumitru, T.A., Miller, E.L., and Farley, K.A., 2000, Post-15 Ma westward structural and thermal encroachment of Basin and Range type extension into the northern Sierra Nevada: Geological Society of America Abstracts with Programs, v. 32, no. 7, p. A43.
Thatcher, W., G.R. Foulger, B.R. Julian, J. Svarc, E. Quilty, and G.W. Bawden, 1999. Present-Day Deformation Across the Basin and Range Province, Western United States. Science, Vol. 283.
Toppozada, T.R., Real, C.R., and Parke, D.L., 1981, Preparation of isoseismal maps and summaries of reported effects for pre-1900 California earthquakes: California Division of Mines and Geology Open-File Report 81-11 SAC, 182 p.
Turner, H.W., 1987, Description of the Downieville quadrangle, California: U.S. Geological Survey Geological Atlas of the United States, Folio 37, scale 1:125,000.
Unruh, J.R., 1991, The uplift of the Sierra Nevada and implications for late Cenozoic epeirogeny in the western Cordillera: Geological Society of America Bulletin, v. 103, p. 1395-1404.
Unruh, J.R., Humphrey, J.R., and W.D. Page, 1996. Northwest continuation of the greater Walker Lane Belt and counterclockwise rotation of the Sierra Nevada microplate, northeastern California. Abstracts with Programs - Geological Society of America, vol.28, no.5, pp.119.
U.S. Geological Survey National Earthquake Information Center, World Data Center for Seismology, Internet access.
Ward, S.N., 1990. Pacific-North America plate motions; new results from very long baseline interferometry. Journal of Geophysical Research, B, Solid Earth and Planets, vol.95, no.13, pp.21,965-21,981.
Wernicke, B., Friedrich, A.M., Niemi, N.A., Bennett, R.A., and J.L. Davis, 2000. Dynamics of plate boundary fault systems from Basin and Range Geodetic Network (BARGEN) and geological data GSA Today, vol.10, no.11, pp.1-7.
Wills, C.J. and Borchardt, G., 1993, Holocene slip rate and earthquake recurrence on the Honey Lake fault zone, northeastern California: Geology, v. 21, p. 853-856.

STOP 10

John Wakabayashi, 1329 Sheridan Lane, Hayward, CA 94544, wako@tdl.com,
http://www.tdl.com/~wako/

Overview Point Along Middle Fork-North Fork Yuba River Divide

This overview stop on the Middle Fork-North Fork Yuba River divide allows one to view the late Cenozoic incision of the North Fork Yuba River, in addition to relief that predated this incision (referred to as paleorelief). We park on a ridge that is capped by Tertiary volcanic rocks; our parking spot is near the base of these rocks where they overlie Paleozoic metamorphic rocks. From our parking area we can take a walk down a short logging spur on the north side of this ridge to the base of the volcanic rocks (only 5-7 m lower than where you park). From here one can look northward, down into the North Fork Yuba River canyon. The canyon bottom is about 650 m below this point. This represents the late Cenozoic incision of the North Fork Yuba River into the basement (pre Cenozoic) metamorphic rocks beneath the Tertiary volcanic cover (see Fig. 10-1). Because this area was blanketed with Cenozoic volcanic rocks, the river had to cut through the volcanic rocks and the basement. The maximum age for the start of this stage of incision can be estimated by the age of the youngest of these extensive volcanic deposits. This age is approximately 5 Ma (see discussions in Wakabayashi and Sawyer, 2001; and Unruh, 1991). Relationships between Tertiary units elsewhere in the Sierra, and the tilts of strata along the western margin of the range indicate incision through basement and tilting was minimal prior to 5 Ma. These same relationships indicate that tilting and major stream incision began not long after 5 Ma. Late Cenozoic incision in the Sierra Nevada is shown on Fig. 10-2.

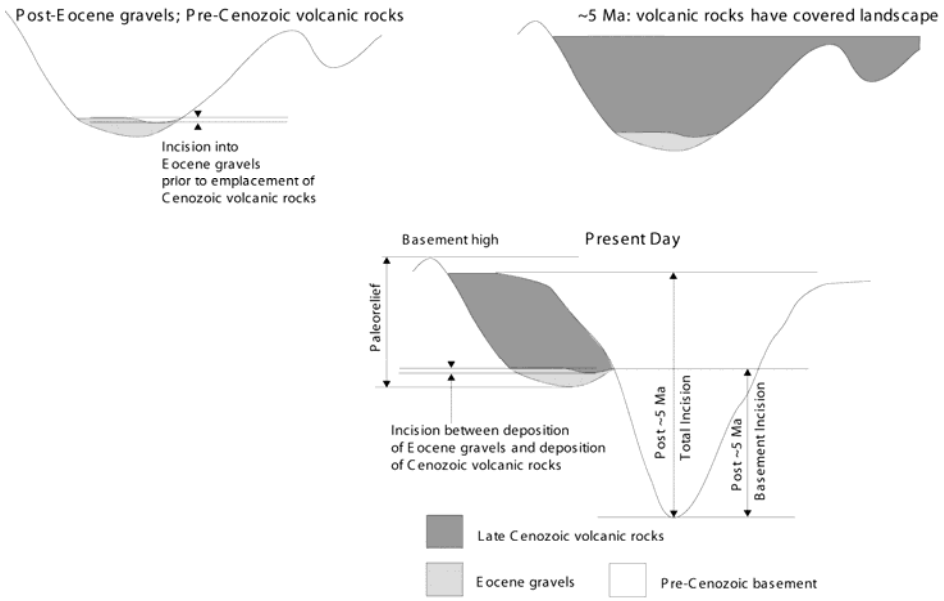

Figure 10-1: Diagram depicting the development of the cross section of a typical Sierra Nevada canyon. At many localities, late Cenozoic volcanic rocks directly overlie basement rather than Eocene gravels. Adapted from Wakabayashi and Sawyer (2001).

Looking northward across the canyon one sees the rugged summit of the Sierra Buttes, composed of Paleozoic metamorphic rocks, nearly 800 m higher than where you stand; this is the minimum amount of local relief represented by the Sierra Buttes at the time of the deposition of the volcanic rocks (paleorelief). The Sierra Buttes are the highest of several isolated basement highs in the northern Sierra. Other basement highs can be seen south of our viewpoint; some may be visible from south side of the ridge we are on, whereas others are visible on the drive to and from Highway 89. These paleorelief highs

include the Grouse Ridge area (about 500 m of paleorelief) and English Mountain, south of Jackson Meadow Reservoir (about 600 m of paleorelief). In general, there is little paleorelief in the northern Sierra except for these isolated highs (Fig. 10-3). In contrast, the Sierra Nevada from Yosemite southwards has a large amount of paleorelief. The bounding ridges of the San Joaquin River drainage, for example, have summits over 1000 m (locally over 1500 m) higher than the position of the 10 Ma ancestral San Joaquin River channel of Huber (1981).

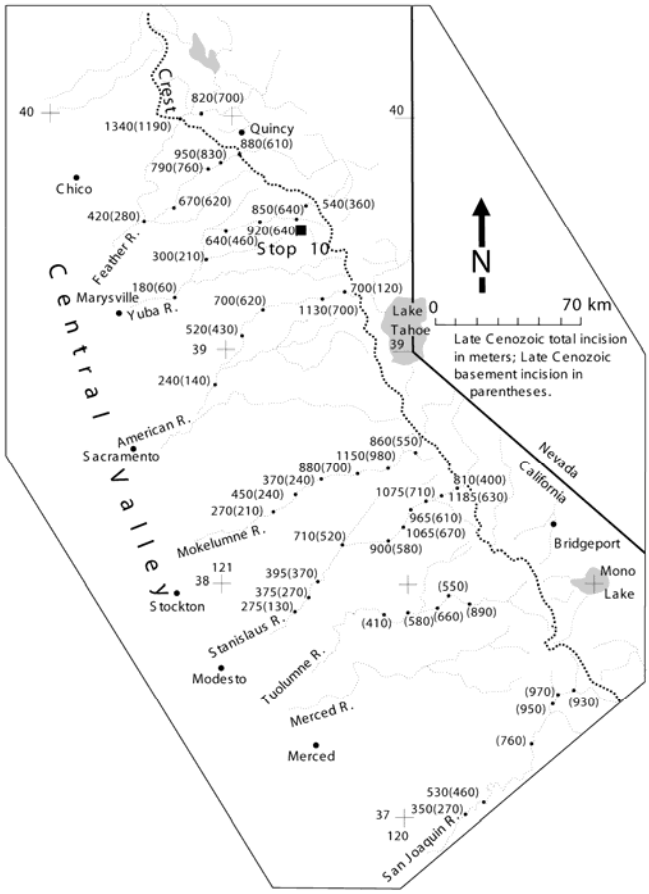

Figure 10-2. Late Cenozoic stream incision of the northern and central Sierra Nevada. Adapted from Wakabayashi and Sawyer (2001).

Stream incision and paleorelief offer clues to the long-term topographic evolution of the Sierra Nevada. Uplift of the range, however, cannot be evaluated unless there are features that can be tied to absolute elevation. In the Sierra Nevada the hingeline area (Fig. 10-4) has stayed at about the same elevation relative to sea level throughout the late Cenozoic (e.g., Huber, 1981; Unruh, 1991). Thus, well-preserved late Cenozoic units, such as the Lovejoy basalt and Table Mountain latite, can be used to record deformation, tilting, and rock uplift across the Sierra Nevada (Wakabayashi and Sawyer, 2000; 2001). The valleys down which the Lovejoy basalt and Table Mountain latite and other units flowed had lower gradients than the modern rivers. These paleovalleys were broad and alluviated in contrast to the narrow, deep canyons associated with today's rivers. Very low incision rates of streams from Eocene to Miocene time, recorded by the channeling of Miocene and/or Oligocene units through Eocene units are consistent with low stream gradients (Wakabayashi and Sawyer, 2001). Some estimates for ranges of paleogradients can be made for the drainages down which units such as the Lovejoy basalt and Table Mountain latite flowed; such estimates can be used with the present day configuration of well-preserved late Cenozoic units to estimate rock uplift in the Sierra (Fig. 10-4) (Wakabayashi and Sawyer, 2001). Late Cenozoic (post ~5 Ma) rock uplift of the Sierra Nevada is estimated at about 1700-1900 m. Erosion of bedrock summit flats in the Sierra has been very low (Small et al.,1997), so the uplift for the Sierra crest area, estimated from reconstructed late Cenozoic units approximates surface uplift for those summit

areas (Fig. 10-4). The fastest long-term late Cenozoic erosion rates are recorded by the most deeply incised parts of the modern canyons. Incision in such canyons can be compared to the rock uplift calculated for that area. Such an analysis shows that even the rocks at bottom of the deepest canyons have experienced surface uplift of 600-1100 m (schematically shown in Fig. 10-4) (Wakabayashi and Sawyer, 2001). Thus, there has been considerable mean surface uplift of the range in the late Cenozoic.

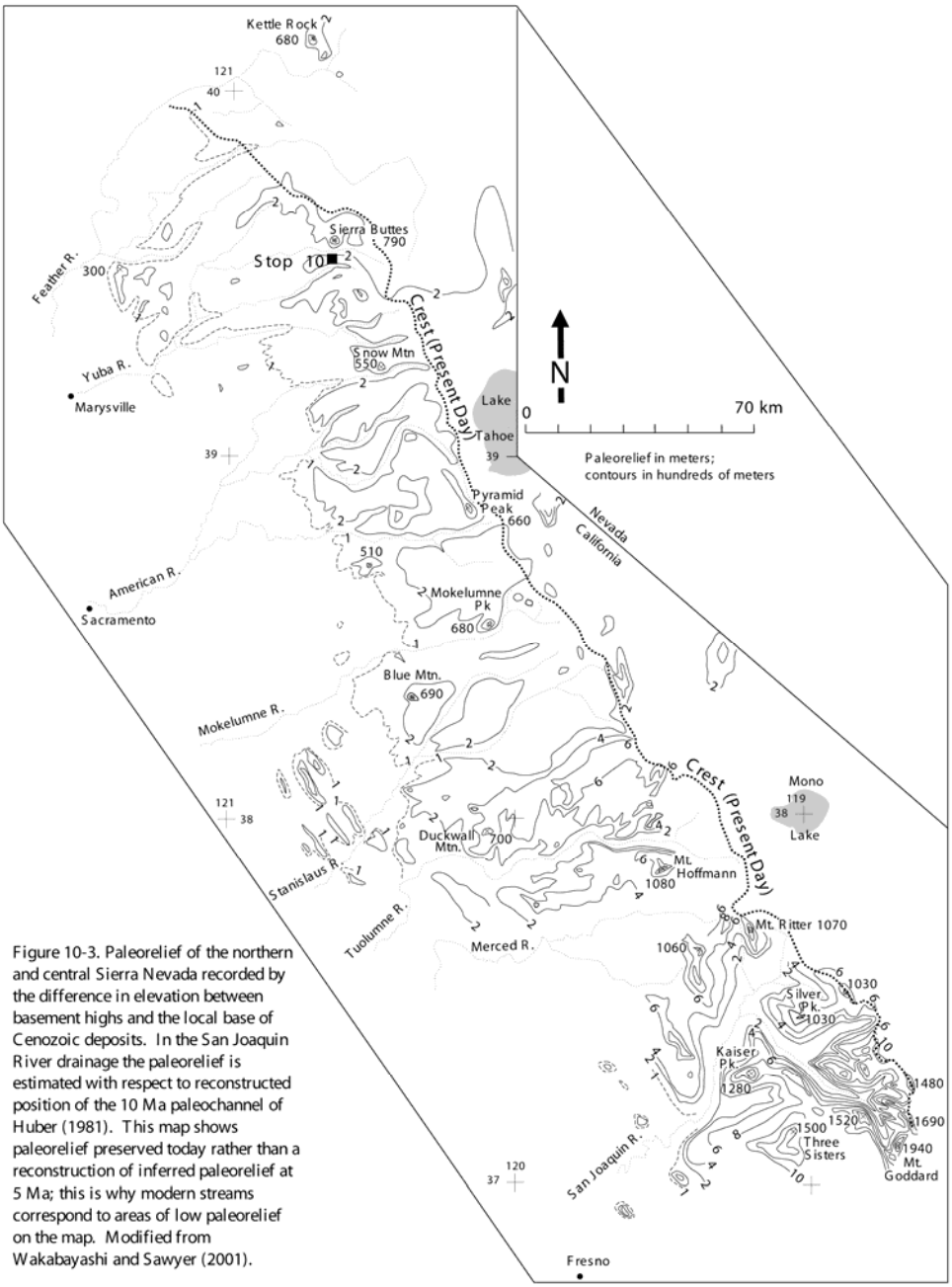

Figure 10-3. Paleorelief of the northern and central Sierra Nevada recorded by the difference in elevation between basement highs and the local base of Cenozoic deposits. In the San Joaquin River drainage the paleorelief is estimated with respect to reconstructed position of the 10 Ma paleochannel of Huber (1981). This map shows paleorelief preserved today rather than a reconstruction of inferred paleorelief at 5 Ma; this is why modern streams correspond to areas of low paleorelief on the map. Modified from Wakabayashi and Sawyer (2001).

The lack of Miocene-Eocene stream incision is associated with a lack of tilting and inferred Miocene-Eocene rock uplift. Eocene gravels underlie the late Cenozoic deposits throughout the northern and central Sierra, even in the Sierra crestal area. If significant Eocene-Miocene rock uplift and tilting had occurred, then Eocene deposits near the Sierran crest should be present as perched remnants high above the base of Miocene deposits. The Eocene deposits beneath Miocene and Oligocene volcanic rocks include exposures across (north) the North Fork Yuba River canyon from our viewpoint both upstream (east) and downstream (west) of Sierra Buttes. These exposures include deposits beneath Haskell Peak

that is on the crest of the range. The lack of significant rock uplift and stream incision between Eocene and Miocene time suggests that paleorelief we see today was created prior to the Eocene (Wakabayashi and Sawyer, 2001).

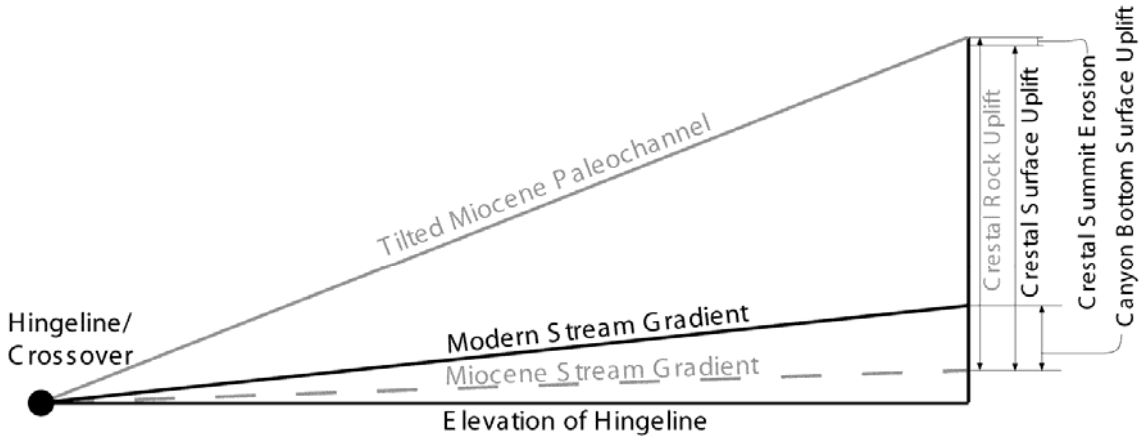

Fig.10-4: Diagram showing the relationship between tilted Tertiary paleochannels, Miocene stream gradients, and surface and rock uplift. Adapted from Wakabayashi and Sawyer (2001).

There has been considerable debate about whether or not late Cenozoic uplift occurred in the Sierra (e.g., Huber, 1981; Unruh, 1991; House et al., 1998; Wakabayashi and Sawyer, 2001), and what tectonic or other mechanisms influenced the topographic development of the Sierra Nevada (e.g., Small and Anderson, 1995; Wakabayashi and Sawyer, 2001); much of this debate is discussed in Wakabayashi and Sawyer (2001) and references therein. This final stop of the FOP trip affords a great backdrop to discuss various models for the evolution of California's most prominent mountain range.

References

House, M.A., Wernicke, B.P., and Farley, K.A., 1998, Dating topography of the Sierra Nevada, California, using apatite (U-Th)/He ages: Nature, v. 396, p. 66-69.

Huber, N.K., 1981, Amount and timing of late Cenozoic uplift and tilt of the central Sierra Nevada, California-evidence from the upper San Joaquin river basin: U.S. Geological Survey Professional Paper 1197, 28p.Wakabayashi, J., and Sawyer, T.L., 2001, Stream incision, tectonics, uplift, and evolution of topography of the Sierra Nevada, California: Journal of Geology, v. 109, p. 539-562.

Small, E.E., and Anderson, R.S. 1995, Geomorphically driven late Cenozoic rock uplift in the Sierra Nevada, California: Science, v. 270, p. 277-280.

Small, E.E.; Anderson, R.S.; Repka, J.L.; and Finkel, R. 1997. Erosion rates of alpine bedrock summit surfaces deduced from in situ 10Be and 26Al. Earth Planet. Sci. Lett. 150: 413-425.

Unruh, J.R., 1991, The uplift of the Sierra Nevada and implications for late Cenozoic epeirogeny in the western Cordillera: Geological Society of America Bulletin, v. 103, p. 1395-1404.

Wakabayashi, J., and Sawyer, T.L., 2000, Neotectonics of the Sierra Nevada and the Sierra Nevada-Basin and Range Transition, California, with field trip stop descriptions for the northeastern Sierra Nevada: in Brooks, E.R., and Dida, L.T., eds., Field guide to the geology and tectonics of the northern Sierra Nevada, California Division of Mines and Geology Special Publication 122, p. 173-212.

Wakabayashi, J., and Sawyer, T.L., 2001, Stream incision, tectonics, uplift, and evolution of topography of the Sierra Nevada, California: Journal of Geology, v. 109, p. 539-562.